Journal Homepage: https://dergipark.org.tr/tr/pub/isibted

Isı Bilimi ve Tekniği Dergisi

Archive: https://tibtd.org.tr/dergi

CFD-Based Calibration of Representative Elementary Units for Dry Pressure Drop in Structured Packings

Volkan TOPALOĞLU [1, *], Hakan DEMİR[1]

[1] *Yildiz Technical University, Faculty of Mechanical Engineering, Department of Mechanical Engineering, 34349 Besiktas, İstanbul, Türkiye*

A R T I C L E I N F O

2026, vol. 46, no.1, pp. 167-175

doi: 10.47480/isibted.1833958

Research Article
Received: 07 December 2025
Accepted: 03 March 2026

* *Corresponding Author*
e-mail: volkant@outlook.com

Keywords:
Separation process
structured packing,
dry pressure drop,
representative elementary unit,
computational fluid dynamics

ORCID Numbers in author order:
0009-0001-1675-745X
0000-0002-6891-0831

A B S T R A C T

Representative Elementary Unit (REU) simplification has become a standard approach for CFD modeling of structured packings; however, its reliability in predicting dry pressure drop remains a critical yet underexplored issue. In particular, the sensitivity of hydraulic performance to internal geometric parameters is often overlooked in the current literature. This study addresses this gap by calibrating an REU model for Mellapak 500.Y against the semi-empirical correlation of Stichlmair et al. (1989) and experimental data from Tsai (2010). Single-phase simulations were conducted using the SST k–ω turbulence model over a gas-load range of 0.72–4.32 $Pa^{0.5}$. Grid independence was established at 0.53 million cells per REU. A domain-sensitivity analysis using one, four, and six REUs yielded deviations below 10%, confirming that a single-unit domain provides sufficient accuracy for dry-flow calibration. The results show that the nominal 2.00 mm sheet spacing leads to substantial underprediction of pressure drop, whereas an effective spacing of 0.24 mm brings the CFD predictions into agreement with Tsai's measurements within a ±20% error band and consistent with the Stichlmair correlation across the operating window. These findings identify the effective sheet spacing as the dominant geometric calibration parameter and provide a reproducible, computationally efficient baseline REU for subsequent hydrodynamics simulations in Mellapak 500.Y.

Yapılandırılmış Dolgularda Kuru Basınç Düşümü için Temsili Eleman Birimlerinin CFD Tabanlı Kalibrasyonu

M A K A L E B İ L G İ S İ

Anahtar Kelimeler:
Ayırma prosesi,
yapılsal dolgu,
kuru basınç kaybı,
temsili eleman hücresi,
hesaplamalı akışkanlar dinamiği,

Ö Z E T

Temsili Eleman Birimi (TEB, Representative Elementary Unit - REU) sadeleştirmesi, yapılandırılmış dolguların CFD ile modellenmesinde standart bir yaklaşım hâline gelmiştir; ancak kuru basınç düşüşünü öngörmedeki güvenilirliği hâlen kritik ve yeterince incelenmemiş bir konu olarak kalmaktadır. Özellikle, hidrolik performansın iç geometrik parametrelere olan duyarlılığı mevcut literatürde sıklıkla göz ardı edilmektedir. Bu çalışma, Mellapak 500.Y için geliştirilen bir REU modelinin, Stichlmair ve arkadaşlarının (1989) yarı-ampirik korelasyonu ve Tsai'nin (2010) deneysel verileri ile kalibre edilmesi yoluyla bu boşluğu doldurmayı amaçlamaktadır. Tek fazlı akış simülasyonları, 0.72–4.32 $Pa^{0.5}$ gaz yükü aralığında SST k–ω türbülans modeli kullanılarak gerçekleştirilmiştir. Ağ bağımsızlığı, REU başına 0.53 milyon hücrede sağlanmıştır. Bir, dört ve altı REU kullanılarak yapılan alan-duyarlılık analizi, %10'un altında sapmalar vermiş ve tek birimlik bir hesaplama alanının kuru akış kalibrasyonu için yeterli doğruluk sağladığını doğrulamıştır. Elde edilen sonuçlar, nominal 2.00 mm sac aralığının basınç düşüşünün önemli ölçüde düşük tahmin edilmesine yol açtığını; buna karşılık 0.24 mm'lik etkin aralığın, CFD tahminlerini Tsai'nin ölçümleriyle ±%20 hata bandı içinde uyumlu hâle getirdiğini ve tüm işletme aralığında Stichlmair korelasyonu ile tutarlılık sağladığını göstermektedir. Bu bulgular, etkin sac aralığının baskın geometrik kalibrasyon parametresi olduğunu ortaya koymakta ve Mellapak 500.Y için sonraki hidrodinamik simülasyonlarda kullanılabilecek, tekrarlanabilir ve hesaplama açısından verimli bir temel REU modeli sunmaktadır.

NOMENCLATURE

F_G	Gas load, ($Pa^{0.5}$)
U_G	Superficial gas velocity, (m/s)
ρ_G	Gas Density (kg/m^3)
u	Velocity vector (m/s)
p	Static Pressure (Pa)
H	Packing height of the computational domain (m)
g	Gravitational acceleration vector (m/s^2)
μ	Molecular dynamic viscosity (Pa·s)
μ_t	Turbulent dynamic viscosity (Pa·s)
T_{ref}	Reference temperature
μ_{eff}	Effective dynamic viscosity (Pa·s)
k	Turbulent kinetic energy (m^2/s^2)
ω	Specific turbulence dissipation rate (s^{-1})
Δp	Pressure drop across computational domain (Pa)
$\Delta p_{\text{CFD}}(F_G)$	Pressure drop predicted from CFD (Pa)
$\Delta p_{\text{corr}}(F_G)$	Pressure drop from the correlation (Pa)
$\varepsilon_{\Delta p}(F_G)$	Relative error of CFD pressure drop with respect to the correlation
y+	Dimensionless wall distance (-)
R_{air}	Gas Constant for Air ($J\ kg^{-1}K^{-1}$)
$\boldsymbol{\mu_{ref}}$	Reference viscosity (Pa·s)

INTRODUCTION

Distillation is widely recognized as the most energy-intensive separation process in the chemical and process industries, typically accounting for around 40% of the total operational energy input (Kiss & Smith, 2020). This substantial demand is estimated to represent nearly 3% of global energy consumption, which creates a strong incentive to improve separation efficiency through better internals and more reliable design methods (Czarnecki, 2024). In both distillation and absorption service, column performance is still governed to a large extent by the internal geometry, which must simultaneously provide sufficiently high interfacial area and stable wetting for mass transfer, adequate capacity before loading/flooding, and low pressure drop to reduce blower/compressor.

Bed-scale Hydraulics and Correlation-based Design

Among the available internals, corrugated structured packings have become a standard choice for energy-intensive separations because they offer a large specific surface area at comparatively low hydraulic resistance (Sulzer Chemtech, 2003; Aroonwilas et al., 2001). Their periodic geometry promotes efficient gas–liquid contact while limiting the driving power for blowers and compressors, and a large body of experimental work has quantified holdup, wetting and mass-transfer behavior in Mellapak-type packings (Suess & Spiegel, 1992; Tsai, 2010; Wehrli et al., 2018; Schug, 2018). However, most industrial design methods still rely on empirical correlations that embed geometrical effects into a small number of fitting parameters, which makes it difficult to extrapolate these correlations to modified or novel packing geometries (Flagiello et al., 2021). In contrast, recent studies have demonstrated that high-fidelity CFD models can directly capture geometry-dependent hydrodynamics and inform new predictive correlations without relying solely on empirical fitting (Ataki & Bart, 2006).

In parallel with these developments, an extensive body of experimental work has characterized the hydraulic behavior and pressure-drop performance of corrugated structured packings under both dry and irrigated conditions. Rocha et al. (1993) combined new air–water measurements for Mellapak-type packings with literature data to formulate a mechanistic model that links pressure drop and flooding to liquid holdup through effective film thickness and channel geometry, and showed that small variations in corrugation angle and surface treatment can noticeably shift the loading point and ΔP profile. Billet and Schultes (1993) likewise developed a widely used semi-empirical framework in which friction factors and volumetric mass-transfer coefficients are correlated to holdup and specific surface area, implicitly embedding the dependence of dry and wet pressure drop on packing geometry. Complementary large-scale column tests by Olujić and co-workers demonstrated that pressure drop is highly sensitive to column diameter and corrugation layout: for Montz B1-250, ΔP per unit height decreases and capacity increases as the column diameter becomes large relative to the packing element height, while geometric refinements at layer interfaces add additional capacity without sacrificing efficiency (Olujić, 1999; Olujić et al., 2003). More recently, Tsai (2010) reported a comprehensive database of hydraulics for several Mellapak geometries, including dry-gas and irrigated pressure-drop measurements over wide ranges of liquid load, surface tension, and viscosity, and used these data to benchmark hydraulic models such as those of Rocha et al. (1993) and the generalized pressure drop correlation (GPDC). Collectively, these studies have consolidated a large experimental hydraulic database that enables bed-scale performance prediction and practical sizing of distillation and absorption columns. In recent years, this baseline has also been used to benchmark CFD studies, allowing order-of-magnitude estimates of key hydraulic metrics.

Structure-resolved CFD

Rapid advances in high-performance computing (HPC) have enabled structure-resolved CFD to become a viable and increasingly influential methodology for understanding packing-scale hydrodynamics. Early CFD studies on structured packings focused on wetting behavior and local film/rivulet dynamics on individual elements (Ataki & Bart, 2006; Shojaee et al., 2012), while more recent work has systematically investigated the influence of perforations, surface characteristics and flow conditions on liquid holdup and interfacial area (Singh et al., 2018, Singh et al., 2020; Ambekar et al., 2024). In parallel, Isoz and Haidl (2018) provided high-resolution experimental evidence that subtle variations in channel geometry can induce measurable changes in gas distribution, thereby emphasizing the intrinsic geometric sensitivity of structured-packing hydrodynamics. Similarly, Li et al. (2016) and Sun et al. (2021) demonstrated that CFD-based, multi-scale analyses enable rapid and cost-effective screening of novel corrugated structural packing geometries before fabrication, allowing hydraulic performance to be predicted and compared without capital intensive prototyping or experimental campaigns.

REU-based Hydrodynamics

To ensure computational tractability, contemporary CFD studies commonly leverage the inherent periodicity of corrugated-sheet packings and employ a REU framework, wherein a minimal geometrical segment is simulated under periodic boundary conditions while preserving the dominant hydrodynamic features (Olenberg & Kenig, 2017; Wang et al., 2020; Macfarlan, 2021). This approach renders CFD simulations feasible by focusing on a small, representative unit rather than resolving the entire column, while retaining the key flow physics.

Within the REU framework, Singh et al. (2018) systematically varied solvent property groups (e.g., Ka), liquid load, and static contact angle, showing that interfacial area and liquid holdup increase for more viscous liquids (lower Ka) and decrease as the contact angle increases. Using countercurrent VOF in an REU of Mellapak 250.Y, Singh et al. (2020) incorporated dynamic contact angle and initial wetting, finding 10% shifts in predicted interfacial area, with wetting-history effects generally diminishing at higher liquid loads. More recently, Bertling (2023) showed that sheet perforations can materially reshape local film/rivulet pathways and wetted-area predictions, and Ambekar et al. (2024) demonstrated that explicitly resolving perforations in a periodic REU leads to measurable changes in liquid spreading and film/droplet behavior.

Although liquid holdup and wettability-driven hydrodynamics have been studied extensively within the REU framework, REU-scale investigations of dry pressure drop remain scarce, and many of the studies cited above do not report pressure-drop data. As a result, the sheet-to-sheet gap distance has not been addressed systematically, since the sensitivity of predicted dry pressure drop to REU geometry is seldom examined. Overall, despite these advances, there is still no widely accepted framework for systematically calibrating REU-scale CFD models of structured packings against hydraulic measurements.

Scope and Contribution

This article frames REU-based dry pressure-drop modeling as a methodological calibration problem: we propose a reproducible CFD workflow to calibrate a structure-resolved REU model of Mellapak 500.Y for single-phase dry-gas pressure drop.

We address a key gap in REU-focused dry-hydraulics studies by reframing dry pressure-drop modeling as a calibration problem rather than a one-off case match. Specifically, we test the central question motivating this work: to what extent can REU-scale RANS deliver predictable dry pressure-drop responses when the geometry is transparently anchored to measured ΔP data? Because dry pressure drop is experimentally accessible and strongly governed by packing geometry, an explicit geometry-to-ΔP anchoring strategy provides a clear baseline and reduces reliance on manual trial-and-error tuning.

Methodologically, we start from a multi-REU domain previously used to reproduce literature dry ΔP trends and build a reusable workflow. We first establish numerical credibility by evaluating mesh refinement, near-wall prism-layer treatment, and domain-length representativeness (via 1-, 4-, and 6-REU domains) to identify a practical reference setup and the minimum length required for a stable unit pressure drop. We then complete the calibration step by varying the normal sheet-to-sheet spacing and selecting an effective gap that reconciles CFD predictions with the semi-empirical correlation of Stichlmair et al. (1989) and the dry pressure-drop data of Tsai (2010). Together, these steps form a reproducible REU calibration recipe for dry hydraulics.

Mellapak 500.Y is selected as a benchmark packing because consistent reference dry-hydraulics data are available (Tsai, 2010) and the packing is widely used in absorption and distillation, providing a clear and relevant baseline for subsequent extensions. Accordingly, the present study is restricted to single-phase dry-gas pressure drop for Mellapak 500.Y, with a non-perforated REU geometry (perforations not explicitly resolved) and RANS closure based on the SST k–ω turbulence model; two-phase hydrodynamics, irrigated pressure drop, and reactive absorption are outside the scope, and the calibrated effective sheet-gap and dry-ΔP response should not be generalized to other packing types without re-calibration against appropriate reference data.

NUMERICAL METHODOLOGY

Gas-Load Definition and Operating Window

The dry pressure drop simulations were performed for single phase gas flow through a REU of Mellapak 500.Y. The operating window was characterized by using the gas load parameter F_G, defined as,

$$F_G = U_G\sqrt{\rho_G} \quad (1)$$

which links superficial gas velocity to the square root of gas density. Here, U_G is the superficial gas velocity based on the empty column area, and ρ_G is the gas density at the case conditions. Expressing the operating range in terms of F_G provides a density-normalized measure of gas throughput, facilitating direct comparison with literature column hydraulics data reported under different gas properties and operating conditions. The selected operating range matches the air-based conditions presented by Tsai (2010) and is summarized in Table 1.

Table 1. Summary of Gas Phase Operations

Gas Load, F_G ($Pa^{0.5}$)	Temperature (°C)	Density ρ_G (kg/m3)	Viscosity $\boldsymbol{\mu}$ (Pa·s)	Superficial Gas Velocity U_G (m/s)	Reynolds Number Re_G (-)
0.719	18.8	1.209	1.810×10^{-5}	0.654	335
1.082	19.5	1.206	1.812×10^{-5}	0.985	497
1.444	19.6	1.206	1.812×10^{-5}	1.315	663
1.803	19.4	1.206	1.813×10^{-5}	1.642	839
2.164	19.9	1.205	1.813×10^{-5}	1.971	1006
2.884	22.2	1.195	1.823×10^{-5}	2.638	1328
3.603	25.4	1.182	1.839×10^{-5}	3.314	1636
4.317	30.1	1.164	1.861×10^{-5}	4.001	1922

The investigated range (0.719–4.317 $Pa^{0.5}$) corresponds to the air-based operating conditions reported by Tsai (2010) and spans the transition from laminar to turbulent flow in the inclined packing channels. Air properties (temperature, density and viscosity) were taken from the same reference and treated as uniform and constant because of the low-Mach, isothermal nature of the dry-gas regime. To characterize the flow regime, a gas Reynolds number was evaluated using a packing hydraulic diameter defined by following formula (Billet and Schultes, 1993):

$$d_h = \frac{4\varepsilon}{a_p} \tag{2}$$

where ε is the void fraction, used as 0.96. The packing specific surface area (a_p) is 500 $m^2\,m^{-3}$ for Mellapak 500.Y. The Reynolds number was computed as:

$$Re_G = \rho_G U_G d_h / \mu_G \tag{3}$$

The operating conditions and Reynolds number are summarized in Table 1. Based on the channel hydraulic diameter d_h and the operating window, the corresponding channel Reynolds number is between 321 and 1863, indicating predominantly transitional flow regime within the corrugated passages.

Geometric Representation and Computational Domains

Figure 1 presents a single corrugated packing element represented through a repeating unit cell having a vertical height of 11.25 mm and a corrugation spacing of 8.0 mm, corresponding to the geometry of Sulzer Mellapak 500.Y. Each ridge is formed by two inclined surfaces that meet at a 45° channel angle, while a bend radius of 1.0 mm at the crest provides a smooth transition between the adjoining facets (Bertling 2023).

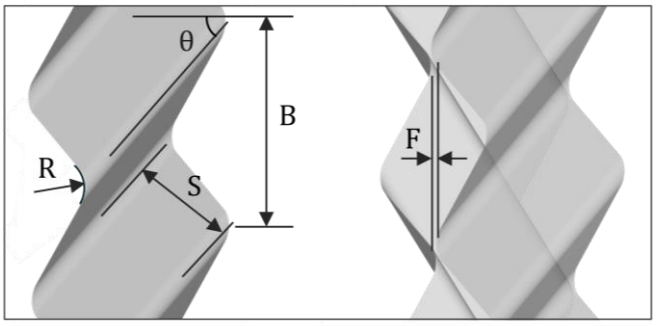

Figure 1. Dimensions defined to represent Sulzer Mellapak 500.Y

A key geometrical parameter in this work is the face-to-face gap between adjacent corrugated sheets. Three sheet spacings were examined: a nominal gap of 2.00 mm that is widely adopted in earlier CFD studies (Singh et al., 2018; Singh et al., 2020), along with narrower calibrated gaps of 0.40 mm and 0.24 mm that yielded substantially improved consistency with reported dry pressure drop measurements in the literature.

In the underlying research, multiple domain lengths (six-REU, four-REU, and single-REU) were considered to assess domain-size effects.

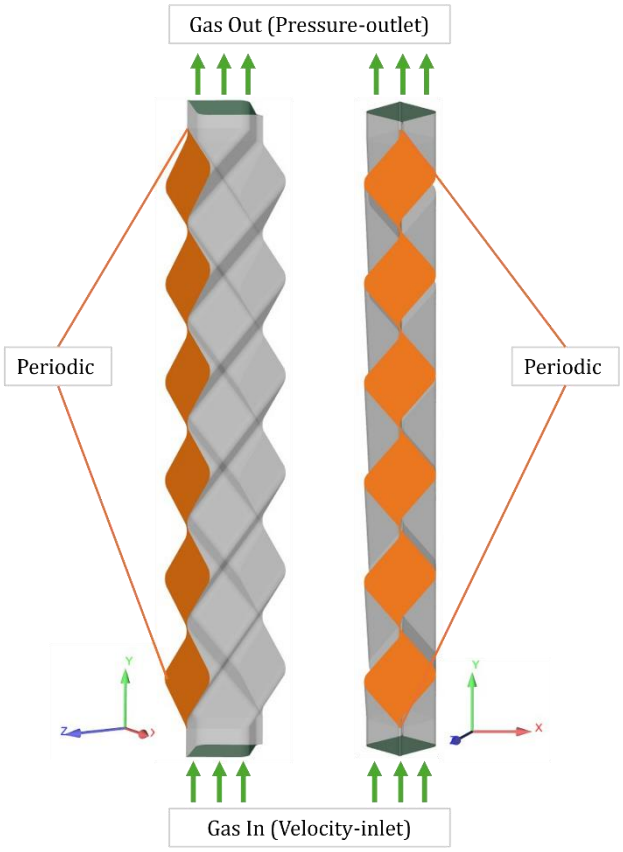

Figure 2. Boundary conditions for the computational domain showing the perspective view (left) and side view (right). Both lateral faces of the domain are treated with periodic boundary conditions.

Mesh Generation

All simulations employed a hex-dominant unstructured mesh generated in ANSYS Fluent (2024 R2). A surface triangular skin was first created on the corrugated sheet walls, followed by insertion of a hex-core region that transitions smoothly to triangular elements. This meshing strategy was chosen to capture the intricate geometry around the corrugation ridges while keeping the total number of cells manageable.

In this study, six different mesh densities were prepared, spanning from a coarse grid to the finest configuration that incorporates multiple prism layers. Table 2 presents the total cell count for each REU along with the corresponding number of prism layers.

Table 2. Number of cells per REU and prism layer configurations with respect to Mesh ID.

Mesh ID	Mesh Name	Cells per REU
M-1	Finest: 8 Prism Layers	$\approx 2.10\ M\ cells/REU$
M-2	Finer: 8 Prism Layers	$\approx 1.10\ M\ cells/REU$
M-3	Fine: No Prism Layers	$\approx 0.53\ M\ cells/REU$
M-4	Fine: 8 and 12 Prism Layers	$\approx 0.49\ M\ cells/REU$
M-5	Medium	$\approx 0.37\ M\ cells/REU$
M-6	Coarse	$\approx 0.10\ M\ cells/REU$

All grids satisfied standard mesh-quality criteria, with minimum orthogonal quality around 0.20, average values close to 0.80, and maximum skewness remaining below 0.70. To further control element stretching, the maximum cell aspect ratio was kept below 20 for meshes employing near-wall prism layers (where high-aspect-ratio cells are expected), while meshes without prism layers were

maintained below 10. In addition, near-wall refinement along the corrugated sheets was sufficiently fine to keep the dimensionless wall distance y+ uniformly small; even for the coarsest grid, the maximum y+ was on the order of two, placing the first cell centers within or very close to the viscous sublayer over the investigated operating conditions.

The SST k–ω turbulence model was selected for its robust near-wall treatment and improved prediction of separation under adverse pressure gradients, which are expected in corrugated packing channels; in the present work it is applied as a two-equation RANS closure (Khosravi Nikou & Ehsani, 2008).

Governing Equations

The dry single-phase gas flow through the Mellapak 500.Y REU was modeled as steady, incompressible and isothermal. Under these assumptions, the governing equations reduce to the Reynolds-averaged Navier–Stokes (RANS) equations for mass and momentum conservation. In compact vector form, the continuity (Eq. 4) and momentum (Eq. 5) equations are:

$$\nabla \cdot (\mathbf{u}) = 0 \tag{4}$$

$$\rho(\mathbf{u} \cdot \nabla)\mathbf{u} = -\nabla p + \rho\mathbf{g} + \nabla \cdot [\mu_{\text{eff}}(\nabla\mathbf{u} + (\nabla\mathbf{u})^T)] \tag{5}$$

The vector $\mathbf{u}$ denotes the mean velocity field, while p represents the mean static pressure. The quantities ρ and μ are the constant gas density and molecular viscosity, respectively, and μ_t is the turbulent viscosity obtained from the SST k–ω model. Effective viscosity is defined as $\mu_{\text{eff}} = \mu + \mu_t$, which combines both molecular and turbulent contributions to the total viscous stress. In the periodically replicated REU used in this study, the gravitational term produces only a uniform hydrostatic gradient along the vertical direction and therefore does not affect the evaluated unit pressure drop; it is retained in the momentum equation for completeness. The resulting set of incompressible RANS equations follows the standard CFD formulation for turbulent single-phase gas flow.

Boundary and Operating Conditions

The simulations adopt a standard REU boundary-condition configuration. At the inlet, a uniform superficial gas velocity was imposed to achieve the desired gas-load parameter for the selected air density as shown in Figure 2. The outlet was specified as a pressure outlet with a fixed zero-gauge pressure.

All corrugated-sheet surfaces were treated as no-slip walls. The lateral faces of the REU were paired and assigned periodic boundary conditions, thereby replicating the repeating nature of the packing and ensuring fully developed flow in the transverse directions.

Each simulation was initialized using the hybrid-initialization routine within ANSYS Fluent 2024 R2. Steady-state convergence was considered achieved when all scaled residuals for continuity, momentum, and turbulence quantities fell below 10^{-3}, and when the monitored pressure drop across the domain exhibited no further variation with iteration. Once converged, the dry pressure drop per REU and the corresponding unit pressure drop were extracted for comparison with literature data and empirical correlations. All simulations were performed using double-precision and second-order spatial discretization schemes (ANSYS, Inc., 2024).

Calibration Strategy and Error Metrics

Dry pressure drop across structured packing was evaluated using the generalized hydraulic correlation of Stichlmair et al. (1989), in the form summarized by Tsai (2010). In the dry-gas limit, the pressure drop per unit packed height is expressed in an Ergun-type equation (Eqs. 6-7) structure:

$$\frac{\Delta p_{\text{corr}}}{H} = f_0 \left[\frac{1-\varepsilon}{\varepsilon^3}\right] \frac{\rho_G U_G^2}{d_p} \tag{6}$$

$$f_0 = \frac{C_1}{Re_G} + \frac{C_2}{Re_G^{0.5}} + C_3 \tag{7}$$

For Mellapak 500.Y, Tsai (2010) reported the packing-specific constants as $C_1 = 12.14$, $C_2 = -0.30$, and $C_3 = 0.49$.

Atmospheric pressure conditions allow the gas-phase properties to be evaluated with standard air-property correlations. Accordingly, the gas density was calculated from the ideal-gas relation (Eq. 8) using the specific gas constant of dry air, R_{air}=287.058 J·kg^{-1}K^{-1} and the measured temperature at each operating point. The dynamic viscosity of air was obtained from Sutherland's law (Eq. 9), adopting the commonly used reference parameters for air: μ_{ref}= 1.716×10^{-5} (Pa·s) at T_{ref} = 273.15K, with the Sutherland constant S=110.4 K. The atmospheric pressure was taken as p=101325 Pa. The operational gas-property values reported in Table 1 were generated using (Eqs. 8-9) and subsequently employed in the dry pressure-drop correlation.

$$\rho_g = \frac{p}{R_{\text{air}}\, T} \tag{8}$$

$$\mu(T) = \mu_{\text{ref}} \left(\frac{T}{T_{\text{ref}}}\right)^{3/2} \frac{T_{\text{ref}}+S}{T+S} \tag{9}$$

For each gas load value F_G the CFD solution provides a pressure drop Δp_{CFD} over the computational domain. This quantity is converted to an equivalent pressure drop per meter of packed height, $\Delta p_{\text{CFD}}/H$, using the geometric height represented by the stack of unit cells, so that it becomes directly comparable with bed scale data and design correlations.

The deviation of the CFD prediction from the semi empirical correlation is quantified by a relative error function defined as (Eq. 10),

$$\varepsilon_{\Delta p}(F_G) = \frac{\Delta p_{\text{CFD}}(F_G) - \Delta p_{\text{corr}}(F_G)}{\Delta p_{\text{corr}}(F_G)} \times 100 \tag{10}$$

In the analysis both the signed error and its absolute value are considered, since the sign indicates whether the CFD model tends to over predict or under predict the reference, while the magnitude reflects the overall agreement. Tsai (2010) and subsequent authors have shown that even for the original experimental data the correlation reproduces the dry pressure drop within a finite scatter that is typically on the order of 10-20%, which defines a practical uncertainty band.

In the present work the goal of the calibration is therefore not an exact match at every operating point, but a consistent alignment of the CFD predictions with the central trend of the correlation and the experimental data across the full gas load range. From this perspective grid independent solutions that remain within the expected error band are considered adequate for subsequent two-phase simulations and parametric studies.

RESULTS AND DISCUSSION

Grid Sensitivity Analysis

Grid independence was assessed by comparing the predicted unit pressure drop with the semi-empirical correlation of Stichlmair et al. (1989) over the full gas-load range (Tsai, 2010). Figure 3 presents the predicted dry unit pressure drop as a function of gas load for a set of meshes with cell counts between 0.7 million and 13.2 million, together with the Stichlmair 1989 correlation as a reference. All simulations reproduce the expected monotonic increase in pressure drop with gas load. Mesh refinement shows that solutions become effectively grid-independent beyond the baseline resolution, as the 3.2M, 3.5M, and 7.1M grids collapse across the operating window, while the coarsest 0.7M grid exhibits the only notable deviation by exceeding 20% at the highest gas loads. Accordingly, a baseline resolution of 0.53 million cells per REU is adopted for the remaining simulations as a compromise between accuracy and computational efficiency.

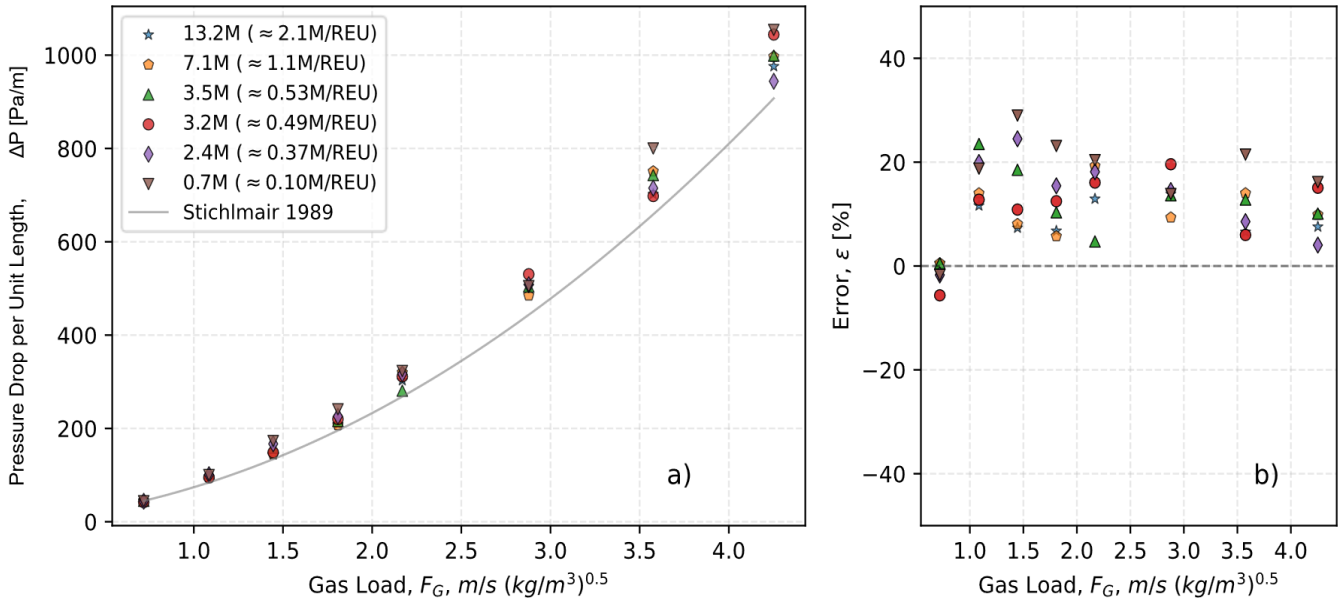

Figure 3. Dry unit pressure drop across the Mellapak 500.Y REU for different mesh densities. Panel (a) compares numerical predictions with the Stichlmair (1989) correlation as a function of gas load F_G. Panel (b) shows the corresponding relative error for each mesh with respect to the correlation.

The grid sensitivity results also reveal a change in the shape of the pressure drop curve around $F_G \approx 0.8$ and 1.0, which can be interpreted as a transition from predominantly laminar to turbulent/transition dominated flow inside the inclined channels. In this region the gas side Reynolds number increases sufficiently for inertial effects to become more important than viscous dissipation, and the ΔP versus F_G curve, so that a relatively small increase in gas load leads to a disproportionately large increase in pressure drop, in line with experimental observations for dry structured packings reported in dry structured packing data (Tsai, 2010).

Number of Prism Layers

Figure 4 investigates the influence of near-wall prism layers on the predicted dry pressure drop in the REU of Mellapak 500.Y. The three meshes have similar total cell counts of about 0.53 million cells per REU but use either no prism layers, eight prism layers, or twelve prism layers adjacent to the solid surfaces. Panel (a) shows that all three meshes reproduce the expected monotonic increase of unit pressure drop with gas load and follow the trend of the Stichlmair correlation over the entire operating window. The relative deviations in panel (b) remain within roughly twenty five percent for every combination of gas load and prism layer setting, and there is no systematic improvement when prism layers are added. Given that the baseline mesh already provides near-wall resolution with y+ on the order of ~1, explicit boundary-layer inflation does not measurably change the predicted dry pressure drop in this REU geometry. This behavior is consistent with prior REU based studies such as Singh (2018) and Isoz and Haidl (2018), where near-wall accuracy is ensured through sufficiently fine global refinement rather than explicit inflation layers. Based on these results, the mesh without prism layers was selected as the reference configuration for the subsequent parametric study, since it delivers essentially the same agreement with the correlation while keeping the mesh generation process simpler. While prism layers are not required for dry-flow calibration at the present resolution, near-wall requirements should be reassessed for future hydrodynamic two-phase simulations where film dynamics and interfacial shear become critical.

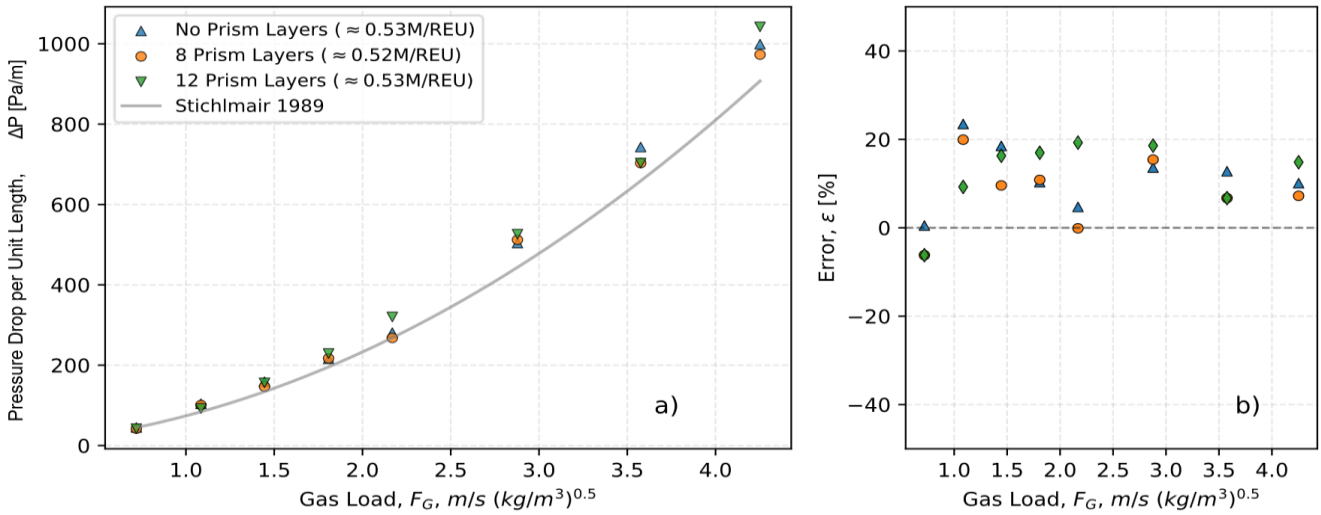

Figure 4. Effect of near-wall prism layers on the predicted dry unit pressure drop across the Mellapak 500.Y REU. Panel (a) compares the numerical pressure drop obtained with meshes that include zero, eight, and twelve prism layers with the semi empirical correlation of Stichlmair et al. (1989) as a function of gas load F_G. Panel (b) reports the corresponding relative deviation of each mesh from the correlation.

Sensitivity to the Number of REUs

Figure 5 examines the influence of the computational domain length, expressed as the number of REUs, on the predicted dry unit pressure drop. Despite the six-fold change in total cell count between the smallest and largest domains, all curves in Figure 5 (a) follow the Stichlmair correlation closely and remain within about 20 percent of it over the investigated range of gas load. Increasing the domain from one to four or six REUs mainly produces a small vertical shift in the pressure drop curve, while the shape and slope with respect to gas load remain essentially unchanged.

The error plot in Figure 5 (b) shows that the relative deviation from the correlation generally lies between 0 and 25 percent and does not exhibit a clear monotonic trend with the number of REUs. At a given gas load the spread between the three configurations is usually below 10%, which is comparable with the scatter reported for dry pressure drop measurements of Mellapak 500.Y. This behaviour indicates that the periodic unit cell assumption is robust and that a single REU already provides a representative description of the dry gas phase hydrodynamics.

From a practical perspective, using only one REU reduces the total cell count by roughly a factor of six compared with the six REU domain, while the improvement in agreement with the correlation is marginal. For the subsequent parametric study, a single REU domain therefore offers a favorable compromise between accuracy and computational cost. Larger domains may be reserved for targeted validation or future two-phase simulations where non-periodic effects (e.g., developing films, flow oscillation or maldistribution) are explicitly investigated.

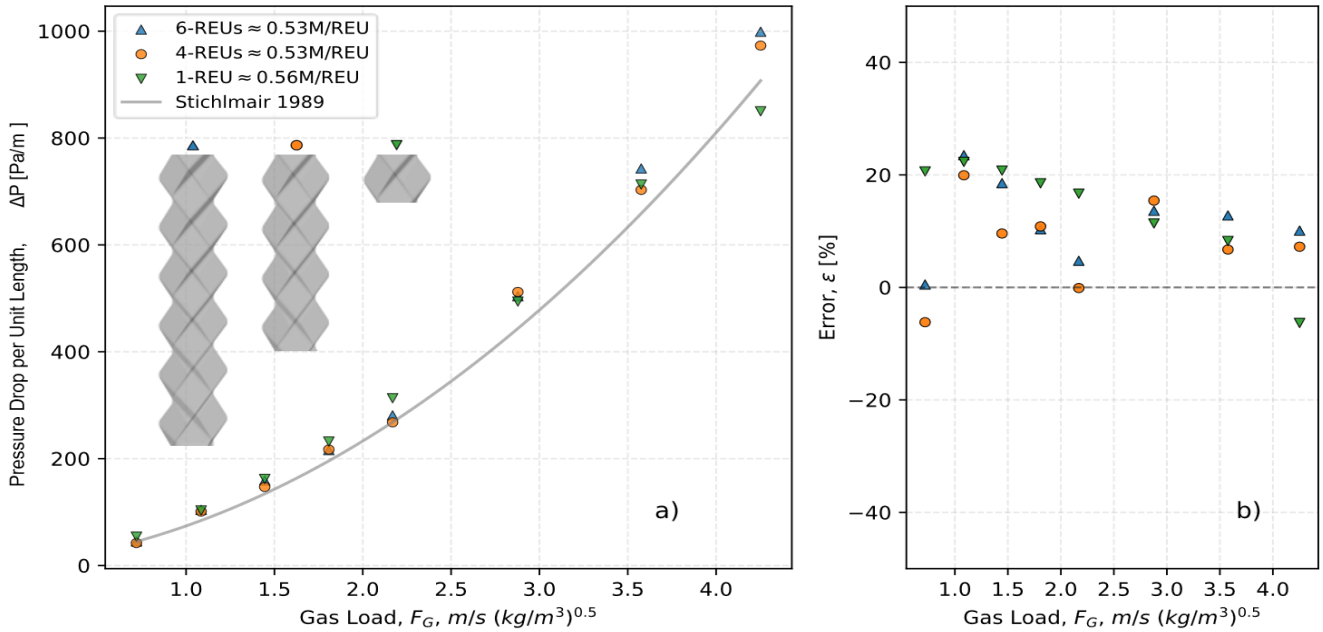

Figure 5. Dry unit pressure drop across Mellapak 500.Y REUs for configurations containing one, four, and six repeating units at similar cell counts per REU. Panel (a) compares numerical predictions with the semi empirical correlation of Stichlmair et al. (1989) as a function of gas load FG. Panel (b) shows the corresponding relative deviation from the correlation.

Effect of Face-to-face Sheet Spacing

Figure 6 shows that all CFD cases reproduce the expected monotonic increase of dry unit pressure drop with gas load. For the smallest effective spacing of 0.24 mm, the numerical predictions follow the dry air experiments of Tsai (2010) over the full operating window and remain close to the Stichlmair (1989) correlation. Agreement is particularly good in the medium and high gas load range, where both the experiments and the correlation indicate a strong increase of pressure drop with F_G.

In contrast, the configurations with larger face-to-face distances display systematically under prediction of the pressure drop. When the spacing is set to 0.40 mm, the simulations still reproduce the qualitative trend but the predicted pressure drops stay below both the experiments and the correlation, with deviations that grow with increasing gas load. The case with the geometrically realistic spacing of 2.00 mm shows the largest discrepancy; at high gas loads the computed pressure drop is roughly a factor of two to three lower than the values suggested in the literature (Stichlmair 1989; Tsai, 2010; Isoz, 2018).

These results identify the effective sheet spacing as the dominant geometric calibration parameter for dry pressure drop in the present REU model. The effective spacing of 0.24 mm can be interpreted as a calibrated value that compensates for unresolved geometric details such as sheet overlap, perforations, local contact points, manufacturing tolerances and surface roughness, which are not represented explicitly in the REU geometry.

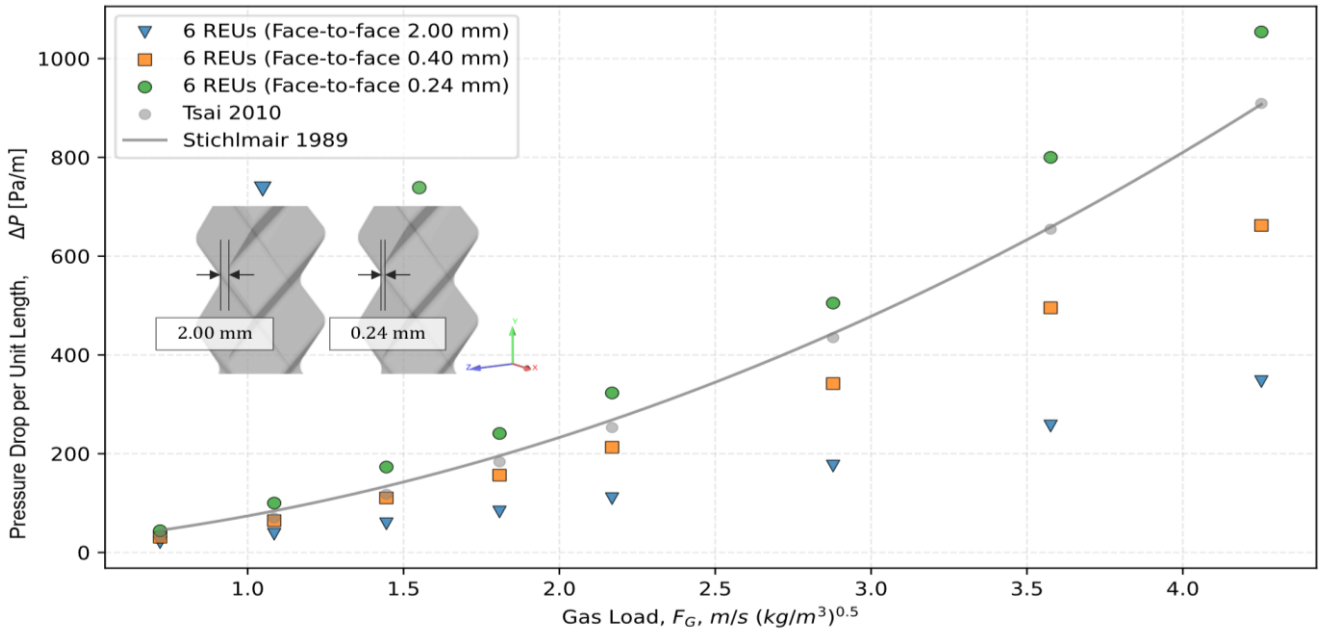

Figure 6. Dry unit pressure drop across six REUs as a function of gas load FG for three face-to-face distances between opposing sheets. Markers show CFD predictions for effective spacings of 2.00, 0.40 and 0.24 mm, while grey circles correspond to the dry pressure drop data of Tsai (2010) and the solid line denotes the Stichlmair (1989) correlation. Insets illustrate the REU geometry and the definition of the normal sheet spacing.

CONCLUSION

In this study a structure resolved CFD model of Mellapak 500.Y was developed and calibrated for dry gas flow through a REU. The gas load range and fluid properties were selected to match the well documented air experiments of Tsai, and the predicted unit pressure drop was systematically compared with the semi empirical correlation of Stichlmair and co-workers. This approach provides a transparent way to link the geometry of the REU to reliable hydraulic data and to remove arbitrary tuning when dry pressure drop is used as the main calibration target.

Numerical verification confirmed that the selected baseline setup (0.53 million cells per REU, no prism layers, single-REU domain) yields pressure-drop predictions that are insensitive to further mesh refinement, near-wall layering, and domain-length extension within the tested range.

Finally, the variation of the face-to-face distance between opposing sheets revealed that the effective normal spacing is the dominant geometrical parameter that controls the dry pressure drop in the present model. An adjusted spacing of 0.24 mm allow the simulations to match both the Stichlmair correlation and Tsai's dry air measurements across the investigated operating window, whereas larger spacings systematically under predict the pressure drop. This calibrated spacing can be interpreted as an effective parameter that accounts for unresolved geometric details. The resulting calibrated REU provides a reproducible and computationally efficient baseline for subsequent two-phase hydrodynamics and reactive-absorption studies in Mellapak 500.Y.

Future work will extend the present dry gas calibration to fully coupled gas–liquid simulations to investigate hydrodynamics, wetting, and mass transfer in Mellapak 500.Y under realistic absorption conditions. In such studies, the calibrated sheet geometry and effective spacing will serve as a fixed geometric baseline, which may help reduce geometric uncertainty and support a clearer interpretation of how flow physics and fluid properties influence holdup, interfacial area, wet pressure drop, and reactive absorption performance.

KAYNAKLAR / REFERENCES

Ambekar, A. S., Peters, E., Hinrichsen, O., Buwa, V. V., & Kuipers, J. (2024). Understanding the role of perforations on the local hydrodynamics of gas–liquid flows through structured packings. Chemical Engineering Journal, 486, 150084. https://doi.org/10.1016/j.cej.2024.150084

ANSYS, Inc. (2024). ANSYS Fluent theory guide: Release 2024 R2. ANSYS, Inc.

Aroonwilas, A., Tontiwachwuthikul, P., & Chakma, A. (2001). Effects of operating and design parameters on CO_2 absorption in columns with structured packings. Separation and Purification Technology, 24(3), 403–411. https://doi.org/10.1016/S1383-5866(01)00140-X

Ataki, A., & Bart, H.-J. (2006). Experimental and CFD simulation study for the wetting of a structured packing element with liquids. Chemical Engineering & Technology, 29(3), 336–347. https://doi.org/10.1002/ceat.200500302

Bertling, J. (2023). Simulation of liquid flow in structured packings using CFD methods. Chemical Engineering Science, 269, 118405. https://doi.org/10.1016/j.ces.2022.118405

Billet, R., & Schultes, M. (1993). Predicting mass transfer in packed columns. *Chemical Engineering & Technology, 16*(1), 1–9. https://doi.org/10.1002/ceat.270160102

Brunazzi, E., Nardini, G., Paglianti, A., & Petarca, L. (1995). Interfacial area of Mellapak packing: Absorption of 1,1,1-trichloroethane by Genosorb 300. *Chemical Engineering & Technology, 18*(4), 248–255. https://doi.org/10.1002/ceat.270180405

Czarnecki, N. J., Giannetti, L., Owens, S. A., Barnicki, S., & Eldridge, R. B. (2024). Energy and economic evaluation of wall placement for divided wall distillation columns. Industrial & Engineering Chemistry Research, 63(43), 18513–18524. https://doi.org/10.1021/acs.iecr.4c01691

Flagiello, D., Parisi, A., Lancia, A., & Di Natale, F. (2021). A review on gas–liquid mass transfer coefficients in packed-bed columns. ChemEngineering, 5(3), 43. https://doi.org/10.3390/chemengineering5030043

Henriques de Brito, M., von Stockar, U., Menendez Bangerter, A., Bomio, P., & Laso, M. (1994). Effective mass-transfer area in a pilot plant column equipped with structured packings and with ceramic rings. Industrial & Engineering Chemistry Research, 33(3), 647–656. https://doi.org/10.1021/ie00027a023

Isoz, M., & Haidl, J. (2018). Computational-fluid-dynamics analysis of gas flow through corrugated-sheet-structured packing: Effects of packing geometry. Industrial & Engineering Chemistry Research, 57(34), 11785–11796. https://doi.org/10.1021/acs.iecr.8b00676

Khosravi Nikou, M. R., & Ehsani, M. R. (2008). Turbulence models application on CFD simulation of hydrodynamics, heat and mass transfer in a structured packing. *International Communications in Heat and Mass Transfer, 35*(9), 1211–1219. https://doi.org/10.1016/j.icheatmasstransfer.2008.05.017

Kiss, A. A., & Smith, R. (2020). Rethinking energy use in distillation processes for a more sustainable chemical industry. Energy, 203, 117788. https://doi.org/10.1016/j.energy.2020.117788

Li, Q., Wang, T., Dai, C., & Lei, Z. (2016). Hydrodynamics of novel structured packings: An experimental and multi-scale CFD study. Chemical Engineering Science, 143, 23–35. https://doi.org/10.1016/j.ces.2015.12.014

Macfarlan, L. H. (2021). *A computational fluid dynamics (CFD)-based investigation of structured packing geometry for gas-phase hydrodynamic and mass transfer performance.* Chemical Engineering Science, [article in press]. https://doi.org/10.1016/j.ces.2021.110844

Olenberg, A., & Kenig, E. Y. (2017). Numerical simulation of two-phase flow in representative elements of structured packings. Computer Aided Chemical Engineering, 40, 2089–2094. https://doi.org/10.1016/B978-0-444-63965-3.50350-0

Olujić, Ž. (1999). Effect of column diameter on pressure drop of a corrugated sheet structured packing. *Chemical Engineering Research and Design, 77*(6), 505–510. https://doi.org/10.1205/026387699526539

Rocha, J. A., Bravo, J. L., & Fair, J. R. (1993). Distillation columns containing structured packings: A comprehensive model for their performance. 1. Hydraulic models. *Industrial & Engineering Chemistry Research, 32*(4), 641–651. https://doi.org/10.1021/ie00016a010

Schug, S. (2018). Untersuchung der fluiddynamik in packungskolonnen mittels computertomographie (Doctoral dissertation). Friedrich-Alexander-Universität Erlangen-Nürnberg.

Shojaee, S., Hosseini, S. H., & Razavi, B. S. (2012). Computational fluid dynamics simulation of multiphase flow in structured packings. Journal of Applied Mathematics, 2012(1), 917650. https://doi.org/10.1155/2012/917650

Singh, R. K., Galvin, J. E., & Sun, X. (2018). Multiphase flow studies for microscale hydrodynamics in the structured packed column. Chemical Engineering Journal, 353, 949–963. https://doi.org/10.1016/j.cej.2018.07.067

Singh, R. K., Bao, J., Wang, C., Fu, Y., & Xu, Z. (2020). Hydrodynamics of countercurrent flows in a structured packed column: Effects of initial wetting and dynamic contact angle. Chemical Engineering Journal, 398, 125548. https://doi.org/10.1016/j.cej.2020.125548

Suess, P., & Spiegel, L. (1992). Hold-up of Mellapak structured packings. Chemical Engineering and Processing: Process Intensification, 31(2), 119–124. https://doi.org/10.1016/0255-2701(92)85005-M

Sulzer Chemtech Ltd. (2003). Structured packings for distillation, absorption and reactive distillation (Brochure reviewed and supplemented in 2002/2003). Sulzer Chemtech Ltd.

Sun, B., Zhang, J., Xie, H., & Zhu, L. (2021). Study on hydrodynamic performance of structured packings for gas–liquid flow: Effects of geometry parameters. *Chemical Engineering Research and Design*, *168*, 318-330. https://doi.org/10.1016/S0263-8762(21)00003-4

Tsai, R. E. (2010). Mass transfer area of structured packing (Doctoral dissertation). The University of Texas at Austin.

Wang, Q., Liu, X., Wu, X., Yang, C., & Qiu, T. (2020). A multi-scale approach to optimize vapor–liquid mass transfer layer in structured catalytic packing. Chemical Engineering Science, 214, 115434. https://doi.org/10.1016/j.ces.2019.115434

Wehrli, M., Kogl, T., Linder, T., & Arlt, W. (2018). An unobstructed view of liquid flow in structured packing. Chemical Engineering Transactions, 69, 775–780. https://doi.org/10.3303/CET1869130